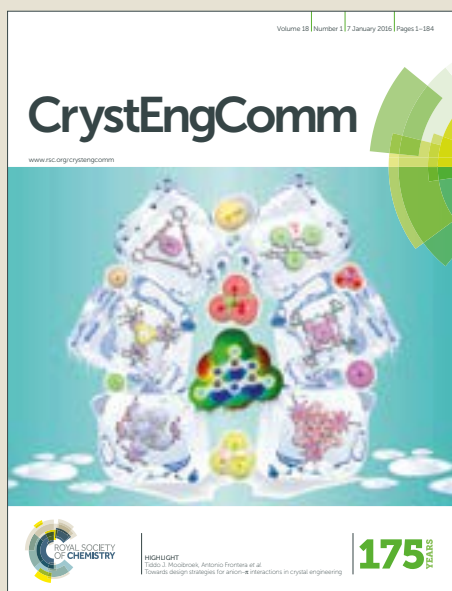


# CrystEngComm

Accepted Manuscript



This article can be cited before page numbers have been issued, to do this please use: L. Kong, H. Wang, S. J. Zhu, H. Zhou and J. Yang, *CrystEngComm*, 2019, DOI: 10.1039/C8CE01940A.



This is an Accepted Manuscript, which has been through the Royal Society of Chemistry peer review process and has been accepted for publication.

Accepted Manuscripts are published online shortly after acceptance, before technical editing, formatting and proof reading. Using this free service, authors can make their results available to the community, in citable form, before we publish the edited article. We will replace this Accepted Manuscript with the edited and formatted Advance Article as soon as it is available.

You can find more information about Accepted Manuscripts in the [author guidelines](#).

Please note that technical editing may introduce minor changes to the text and/or graphics, which may alter content. The journal's standard [Terms & Conditions](#) and the ethical guidelines, outlined in our [author and reviewer resource centre](#), still apply. In no event shall the Royal Society of Chemistry be held responsible for any errors or omissions in this Accepted Manuscript or any consequences arising from the use of any information it contains.

# Understanding the molecular orientation growth at nanometer scale and adjustable electron transition performance of a terpyridyl derivative under different external environments

Received 00th January 20xx,  
Accepted 00th January 20xx

DOI: 10.1039/x0xx00000x

www.rsc.org/

Hai-Yan Wang,<sup>†a</sup> Lin Kong,<sup>†a\*</sup> Shu-Juan Zhu,<sup>a</sup> Hong-Ping Zhou,<sup>a\*</sup> Jia-Xiang Yang<sup>a</sup>

In this study, a terpyridyl derivative 2-(6-(pyridin-2-yl)-4-(4-((E)-2-(pyridin-4-yl)-vinyl)phenyl)pyridin-2-yl)pyridine (abbreviated as PYTPY) has been designed and prepared with A- $\pi$ -A architecture (A = electron acceptor), whose spontaneous aggregation style can be triggered by different external conditions. Mathematical modelling through time dependent density functional theory (TD-DFT) provides a quantitative understanding of the equilibrium molecular geometries at aggregated state between adjacent PYTPY molecules under different additives, such as the addition of water, H<sup>+</sup>, and Ag<sup>+</sup> ion. The vertical electronic excitations and the related UV-vis absorbing character of PYTPY under different conditions were also forecasted, which was verified by the examined absorption spectra. Our method of calculating intermolecular interaction between adjacent molecule, predicting spontaneous aggregation style and absorbing performance under external environment is generally applicable to design and create other functional organic materials.

## 1. Introduction

In the field of materials science, the crystal engineering is an important part, which depends on the understanding of structure-property relationship [1-3]. One of the most relevant issues associated to structure-property relationship study of an organic molecule is the control of self-assembly process, which is required to create functional materials for specific applications. Self-assembly upon spontaneous aggregation of organic molecules turns out to be a very powerful tool that is able to generate supramolecular ordered functionalized structures, formed by spontaneous assembling based on non-covalent interactions. There are two factors that can take effect of a material, one is the intrinsic performance of it [4-5], the other is the conformation of an organic molecule in the bulk scale under different conditions [6]. In this regard, changing the external factors such as pH [7], heat [8], pressure, the introduction of metal ion or guest compound [9], is an attractive prospect to alter the aggregation style and/or properties of an organic material [10-11]. Thus, the studies of external environment on the self-assembly and the related performance of a functional organic compound are at the

forefront of investigations.

2,2':6',2''-terpyridyl derivatives have been demonstrated to be promising candidates for this study because of their unique electronic/optical character and its easily modified structure/performance due to the extensive electronic delocalization [12-13]. Terpyridyl derivatives have gained much interests in the fields of supramolecular, coordination chemistry and material science in the past decade, which show a wide range of potential applications covering light-to-electricity conversion [14], light-emitting electrochemical cells (LECs) [15], (electro)luminescent systems (e.g. organic light-emitting diodes, OLED), nonlinear optical devices [16] and/or life science. The chemical-physical performance of terpyridyl derivatives can be tuned through a careful choice of peripheral substituent groups [17], acid-base medium [18], and/or coordinated metal [19], which are responsible for their aggregation state. Thus, well-designed supramolecular architectures upon terpyridine derivative can be easily realized due to strong metal-terpyridine connectivities [20] and strong hydrogen bond interactions between pyridine and acid medium [21], which open avenues to smart materials with the opportunity of switching the physical and/or chemical characters depending on parameters such as pH value or the existence of metal ions [10]. The self-assembly and the related aggregate style are two main factors that can change the performance of it. Despite tremendous progress in controlling the self-assembly process and the related aggregated structures by electrostatic interactions or stoichiometry method, spatial control of the self-assembly process of such type of terpyridine derivative is still difficult to achieve.

<sup>a</sup> Department of Chemistry, Key Laboratory of Functional Inorganic Materials of Anhui Province, Anhui University, Hefei 230039, P. R. China.

<sup>†</sup> The two authors contributed equally to this work.

<sup>††</sup> \*corresponding author, E-mail: Kong\_lin2009@126.com, zhpzhp@263.net  
Electronic Supplementary Information (ESI) available: [preparation procedure of intermediates 1 and 2; Crystal data of PYTPY; Molecular orbital diagrams of PYTPY monomer and/or dimer at different conditions; Characterization of PYTPY-Ag]. For ESI and crystallographic data in CIF or other electronic format see DOI: 10.1039/x0xx00000x

In this contribution, this study aims to provide a detailed step towards a better understanding of the structure-property relationship between the external condition and self-assembly process of the target terpyridine derivative PYTPY (Figure 1). Pyridine-substituted styrene unit is linked at 4-bit of terpyridine unit to construct A- $\pi$ -A type molecule PYTPY (Scheme 1), which is used to revolute the  $\pi$ -bridge unit that is essential for the molecular engineering. Moreover, extending the  $\pi$ -spacer is useful to enhance the photocurrent for efficient charge transfer [22]. Self-assembly strategies towards  $\pi$ -conjugated terpyridine into advanced supramolecular architectures are evaluated under different external conditions such as water media, the existence of H<sup>+</sup> and/or Ag<sup>+</sup> ions. We start with the aggregate style of PYTPY in dilute tetrahydrofuran (THF) solution under evaporation process (Figure 1). Then different equivalents of H<sup>+</sup> ions are added to change the intermolecular interactions between adjacent molecules, which will then change the orientation aggregate along different directions. Very recently, Spitzer used proton diffusion model to study the assembly process of a dendritic peptide conjugate at a solid-liquid interface [23]. Here, in this study we fix the proton at proper location, N atom at pyridine cycles. Further, Ag<sup>+</sup> ions are introduced into the system to study the changeable intermolecular interactions under strong coordination effect. Based on TD-DFT computations with the B3LYP or BP86 functional (see computational details), its single point energy, structural, electronic and intramolecular charge transfer were successively studied, the computational proposal of which are verified by experimental data. The combined theoretical-experimental approach shows that investigating the self-assembly process is key in manipulating growth direction of aggregated organic structure, and regulating/optimizing the optical performance as well. Our strategy is applicable to many pH/metal ion responsive systems for the preparation of organic aggregates at micro/macro size.

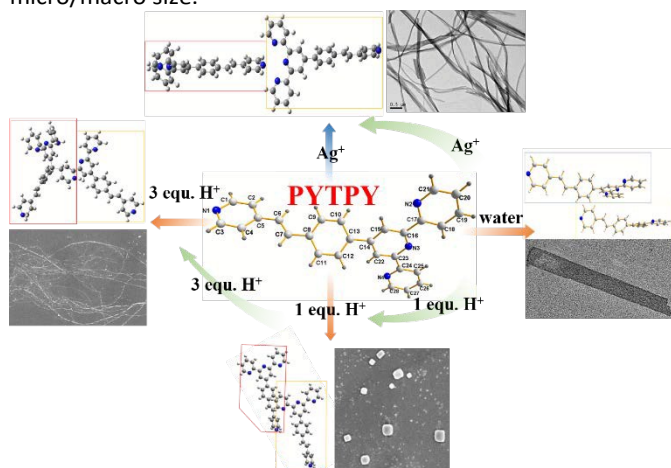


**Figure 1** Illustration of the weak intermolecular interactions and self-assembly structure of PYTPY under different external conditions. At the center: Single crystal structure of PYTPY with the atom numbering.

## 2. Experimental Section

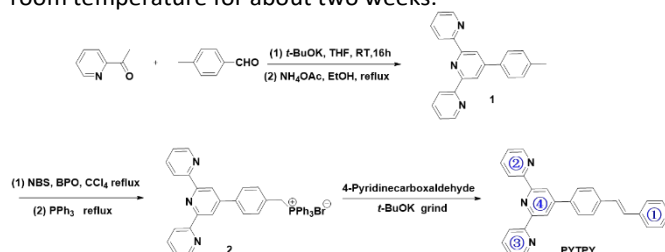
### 2.1 Preparation of PYTPY

View Article Online

DOI: 10.1039/C8CE01940A

The synthesis procedure of intermediates **1** and **2** were listed in ESI. To prepare the target compound PYTPY, intermediate **2** (0.42 g), 4-pyridine formaldehyde (2.00 g) and potassium t-butoxide (*t*-BuOK) (0.50 g) were mixed together and grinded for 30 min. The reaction was monitored by thin-layer chromatography (TLC) to ensure complete reaction. Then, the organic component was dissolved in dichloromethane (CH<sub>2</sub>Cl<sub>2</sub>, 200 mL), washed with saturated salt water for three times, dried overnight with anhydrous magnesium sulfate, removed the organic solvent under rotary evaporation. The residue was purified through column chromatography on silica gel with ethyl acetate used as the eluent to get the target compound as a light-yellow solid. Yield: 30%. <sup>1</sup>H NMR (400 MHz, deuterated chloroform CDCl<sub>3</sub>)  $\delta$  (ppm): 8.78 ~8.73 (m, 4H), 8.69 (d, *J* = 8.0 Hz, 2H), 8.60 (d, *J* = 6.0 Hz, 2H), 7.97 (d, *J* = 8.2 Hz, 2H), 7.89 (td, *J* = 7.8, 1.32 Hz, 2H), 7.68 (d, *J* = 8.2 Hz, 2H), 7.42~7.30(m, 5H), 7.11(d, *J* = 16.3Hz, 1H). <sup>13</sup>C NMR (CDCl<sub>3</sub>, 100 MHz):  $\delta$  = 156.2, 156.0, 150.3, 149.4, 149.2, 144.4, 138.6, 136.9, 136.8, 132.4, 127.8, 127.6, 126.7, 123.9, 121.4, 120.9, 118.0. FI-IR (KBr, cm<sup>-1</sup>): 3054 (m), 1581 (C=N, s), 1457 (C=C, s), 1379 (s), 1040 (m), 800 (s), 724 (s), 658 (m). Ms. Cal: 412.50, Found: 413.25 (M+H<sup>+</sup>).

Light yellow crystals of PYTPY suitable for X-ray diffraction were obtained by slow evaporation of PYTPY-THF solution at room temperature for about two weeks.



**Scheme 1** The preparation procedure of the target PYTPY, four pyridine units were signed as ①, ②, ③, and ④.

### 2.2 Self-assembly of PYTPY in different external conditions

To construct PYTPY aggregates and study the effect of outer condition on the formation, PYTPY was added into water medium with and without acid. Firstly, PYTPY-THF solution was added into water with different water volume ratio ( $f_w$ ). For detail,  $f_w = 90\%$  was described as an example, 200  $\mu$ L of PYTPY-THF solution ( $1.0 \times 10^{-3}$  mol/L) was added into 1.8 mL distilled water under violently stirring for 10 min, then the solution was left undisturbed overnight to let the crystals grow naturally. After that the solution was ultrasonic dispersed for 10 seconds to study the morphology and the UV-vis absorption. Similar experimental methods were used to prepare other samples with the external environment regulated.

Next, a proper  $f_w$  was chosen when different proportions of hydrochloric acid was added to study the influence of acidity on self-assembly process. Upon lowering the pH, the pyridine units were protonated, which in turn induced a monomer to supramolecular aggregation transition.

To study the influence of the coordination effect on the self-assembly, PYTPY-THF solution was added into water with silver

ion, the aggregated morphology and optical performance of which were examined at room temperature. PYTPY@Ag composite was prepared through PYTPY and AgNO<sub>3</sub> in N,N-dimethylformamide (DMF) solution at room temperature under stirring. The PYTPY-Ag complex was prepared in DMF solution at high temperature (140 °C) as well. The two were used as the controlled samples.

### 2.3 TD-DFT calculation

Calculations were carried out *via* TD-DFT method (Gaussian 09). Non-hydrogen atoms were fixed using Cartesian coordinates, and hydrogen atoms were optimized at their most suitable coordinates. Single point energy was calculated at M06/B3LYP method, the detailed level basis for each model was described in the main text. The assembling energy between two relative fragments was defined as  $E_{\text{interaction}} = E_{\text{dimer}} - 2E_{\text{molecule-free}}$  [24]. The electron cloud density distribution of each energy level and the corresponding electron transition were also calculated with bp86 and/or B3LYP method, which was described in the main text along with the level basis.

## 3. Results and discussions

### 3.1 Crystal structure of PYTPY

PYTPY crystallizes in a monoclinic form with space group Cc as shown in the center of Figure 1 with the cell length  $a = 15.8267$ ,  $b = 13.1694$ ,  $c = 10.5443$  and cell angle  $\beta = 106.918^\circ$ . The crystallography data are summarized in Table 1. Selected bond lengths and bond angles are listed in Table S1. In the molecule, the bond lengths of the benzene and pyridine ring are all of aromatic character. The linkage bond length between the benzene ring and the pyridine unit is quite conjugated with C6-C7 being 1.339(4) Å and C13-C14 being 1.492(4) Å. The C6-C7 bond is nearly coplanar to the adjacent benzene and pyridine ring with the torsion angle between C5-C6 and C7-C8 being  $-176.5(3)^\circ$  that is very close to  $180^\circ$ . The adjacent pyridine rings are also nearly coplanar as the torsion angle between C15-C16 bond and C17-C18 bond is  $170.3(3)^\circ$ . Similar result is also observed between C22-C23 bond and C24-C25 bond, with the torsion angle being  $-173.4(3)$ . The structural features reveals that non-hydrogen atoms are highly conjugated and nearly coplanar, which would favor the electronic delocalization in the whole molecule.

There is a C2-H2...N4 intermolecular hydrogen bond with the H2...N4 distance of 2.723 Å ( $\angle\text{C2-H2...N4} = 156.95(22)^\circ$ ) along  $a$  axis as shown in Figure S6a. The adjacent molecules are also stacked through C18-H18...N2 weak interactions along  $c$  axis at a short intermolecular distance of 2.333 Å with the  $\angle\text{C18-H18...N2}$  being  $159.143(192)^\circ$  (Figure S6b). These two types of weak hydrogen bonds are the main driving forces to form one-dimensional (1D) structures (Figure S6). There also exists C3-H3...C27 weak intermolecular interactions with the distance being 2.861 Å and  $\angle\text{C3-H3...C27}$  being  $137.561(234)^\circ$ , which is very important in crystal packing to form two-dimensional sheets in the  $bc$  plane as shown in Figure S7. Further, weak  $\pi$ - $\pi$  interactions between pyridine ring (C4-C5-C2-C1-N1-C3) of one molecule and another pyridine ring (C23-

N1-C16-C15-C14-C22) of adjacent molecule with the distance being 3.8036 Å are contributed to molecular aggregation along  $b$  axis as shown in Figure S8. All these weak interactions are supposed to be the driving forces for the self-assembly to construct into bulk-size and/or micro/nano-size structures.

**Table 1** Crystal data and structure's refinement for PYTPY single crystal

Compound	PYTPY	$V$ [Å <sup>3</sup> ]	2102.5(12)
Formula	C <sub>28</sub> H <sub>20</sub> N <sub>4</sub>	Z	4
Formula weight	412.48	$D_{\text{calcd}}$ [g·cm <sup>-3</sup> ]	1.303
Temperature (K)	296(2)	$\mu$ [mm <sup>-1</sup> ]	0.079
Crystal system	Monoclinic	Limiting indices	-18 $\leq$ h $\leq$ 18 -15 $\leq$ k $\leq$ 15 -13 $\leq$ l $\leq$ 13
Space group	Cc	$F(000)$ Completeness	864 100.0 %
$a$ [Å]	15.827(5)	to theta =	24.99
$b$ [Å]	13.169(5)	$\vartheta$ range [°]	2.05-24.99
$c$ [Å]	10.544(4)	Reflections collected / unique	7243/3228 [R(int) = 0.0459]
$\alpha$ [deg]	90.000	Data / restraints / parameters	3228 / 2 / 290
$\beta$ [deg]	106.918(6)	Final R indices [ $I > 2\sigma(I)$ ]	R1 = 0.0446, wR2 = 0.1002
Crystal size (mm)	0.13 × 0.12 × 0.12	R indices (all data) GOF	$R_1 = 0.0668$ , $wR_2 = 0.1130$ 1.038

### 3.2 Orientation growth and optical performance in water media

#### 3.2.1 Theoretical calculation for orientation growth

It is known that the aggregation structure of a material can be influenced by the external environment of the growth process. However, the intermolecular forces between adjacent molecules is the main cause of the accumulation of a material [25]. Thus, in order to explain the aggregation of PYTPY molecules, firstly, thermodynamic principles are used through computational calculation of weak intermolecular interactions between adjacent molecules by varying the relative position of adjacent molecules and regulation of packing models along  $a$ ,  $b$  and  $c$  axes [26]. The selected fragments were cut out directly from the CIF data, which are listed in Figure 2. The single point energy of free molecule was calculated through b3lyp/6-31g method, which was calculated through b3lyp/6-31g(d) for the dimer. The total energy of the selected fragment and molecule-molecule interaction energy are listed in Table 2. The results shows that the dimer is two times lower in energy than monomer. The energy of intermolecular forces between adjacent molecules along  $a$  axis is 10.66 kJ·mol<sup>-1</sup>, which is 1.83 kJ·mol<sup>-1</sup> along  $b$  axis and 6.40 kJ·mol<sup>-1</sup> along  $c$  axis, respectively. Also, there exists weak  $\pi$ - $\pi$  interaction with the energy being 1.80 kJ·mol<sup>-1</sup>. The relative interaction force along  $a$ ,  $b$ ,  $c$  axis is 1.00: 0.17: 0.60. The results reveal that the interactions along  $a$  axis are stronger than that along the other two, and the interactions along  $a$  and  $c$  directions are much stronger than that along  $b$  axis, which suggests that the interactions between adjacent molecules might lead to one-dimensional (1-D), possibly grew along  $a$  axis due to C2-H2...N4 intermolecular

hydrogen bond) and/or semi two-dimensional (2-D, possibly at *ab* plane) orientation growth in nature (both in micro and macro size). The result is reasonable that there exists multi-types of weak interactions along *a* axis compared to that along the other two, which means that the weak interactions between adjacent molecules along this direction are somewhat stronger than that along the other two. The stronger interaction will lead to spatially oriented growth. Thus, understanding the formational mechanisms of assembly process can be challenging due to these weak interactions at different directions, which generally determines growth directionality so crucial for the rational design and construction of spontaneous aggregation assemblies into both micro and macro sizes. The calculation results give us confidence to predict aggregation style in other external environments.

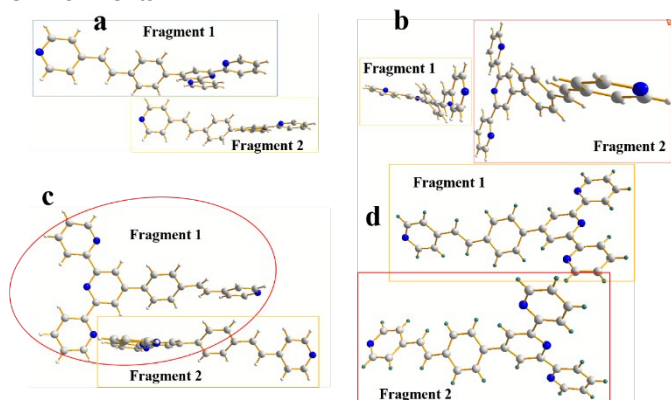


**Figure 2** Fragments selected for calculation of weak interactions along (a) *a* axis, (b) *b* axis, (c) *c* axis, and (d) for very weak  $\pi$ - $\pi$  interactions.

**Table 2** Total, assembling energies of PYTPY molecules along different directions at the M06/6-31+g(d) level

axis	Energy (Hartree)		binding energy $\Delta E$ (kJ/mol)	relative binding energy
	(dimer)	(molecule-free)		
a	-2594.52824098		-10.66	1.00
b	-2594.52346614	-1297.26208380	-1.83	0.17
c	-2594.52661375		-6.40	0.60
$\pi$ - $\pi$	-2594.52485592		-1.80	0.17

$$\Delta E = E_{\text{interaction}} = E_{\text{dimer}} - 2E_{\text{molecule-free}}$$

### 3.2.2 Morphology of aggregated structure formed from THF-H<sub>2</sub>O mixed solvent

In order to verify the influence of intermolecular interactions on molecular aggregation, PYTPY-THF solution was added into water media. Then the aggregated morphology was checked which is shown in Figure 3. It is well known that the self-assembly morphology is related to the solubilization of a compound in a solvent [27]. That is to say, when the compound in a good solvent is added into a bad solvent, a possible aggregated self-assembly structure will be observed, at micro and/or macro sizes [28]. When the concentration of PYTPY is  $1.0 \times 10^{-5}$  mol/L with water volume fraction  $f_w = 90\%$ , well distributed nanorods with length of about 1  $\mu\text{m}$  can be captured in Figure 3a. When the  $f_w$  value is increased to 99%, the rods gather together to form bundle-like structure as shown in Figure 3b. The length of the rod is about 0.7~1.4  $\mu\text{m}$

and the width ranges from 65 nm to 130 nm. The L/D ratio ranges from 9 to ~19, especially in the red-marked circles in Figure 3b. The TEM image of a typical rod is listed in Figure 3c. The results mean that  $f_w$  change do not influence the intrinsic structure, but influences the aggregation degree. Thus, it can be concluded from the calculation results and the experimental observations that the intermolecular interactions between adjacent molecules control the aggregation.

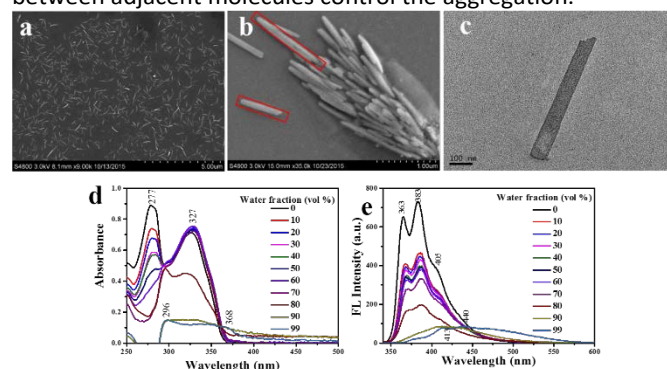


**Figure 3** Morphology of PYTPY nanostructures obtained from THF-H<sub>2</sub>O mixture at the concentration being  $1.0 \times 10^{-5}$  mol/L: (a) SEM image of PYTPY with  $f_w$  being 90%, (b) SEM image of PYTPY as  $f_w$  being 99%, (c) TEM image of a single nanorod as shown in (b). (d) UV-vis absorption and (e) fluorescent emission spectra of PYTPY in THF-H<sub>2</sub>O with tunable water volume fraction

### 3.2.3 Calculated and experimental electron transition performance at monomer state and dimer

The electron transition performance of a compound is dependent on the charge separation between the ground and excited state, which can be influenced by aggregated style [10]. The electron transition can be estimated through the charge-hole distance  $d_{\text{he}}$  between the ground and excited state [29]. To understand the electronic structure and electron transition of PYTPY in diluted THF solution and aggregated state, molecular orbital and energy level distribution calculations of TD-DFT were performed through bp86/cc-pvtz level basis set for both molecule monomer and dimer. The molecular geometry used for the calculation was obtained from X-ray diffraction crystallographic data just as that used for single point energy calculation. As for the dimer, the molecular geometry possessing the lowest energy was chosen just as shown in Figure 3a. The theoretical spectral characteristics (detailed information is listed in Table 3) showed two main transitions as  $\lambda_{\text{abs}} = 325.96$  nm with oscillator strength  $f$  being 0.2516, and  $\lambda_{\text{abs}} = 279.65$  nm with  $f$  being 0.2020, respectively. The lower energy band is transitioned from the HOMO-6 orbit to the LUMO with major contributors  $C_{(\text{HOMO-6})-\text{LUMO}}$  being 0.56068. The higher energy band is from the HOMO-10 orbit to the LUMO with  $C_{(\text{HOMO-10})-\text{LUMO}}$  being 0.43994. In the HOMO-6 and HOMO-10 orbits, the electrons are primarily concentrated on terpyridine unit (Figure S11). In the LUMO orbit, the electrons are primarily concentrated on benzene unit, C=C double bond and pyridine unit ①. The results mean that the electron transition is accompanied by the intramolecular charge transfer performance. Although the PYTPY is a typical A- $\pi$ -A type molecule, the electronic cloud density of terpyridine unit is much higher than that of pyridine unit ① at the other end [30]. When the whole molecule is at the ground state, it is reasonable that the electron cloud may be concentrated at the terpyridine unit and away from the pyridine unit ①. When it is excited, the electron cloud density will be

redistributed. Thus, a weak intramolecular charge transfer from terpyridine unit to pyridine unit ① can be observed when the molecule is excited. As for the fluorescence emission, there exists a main fluorescence band with  $\lambda_{FL} = 380.27$  nm, which results from the transition between the LUMO orbit and the HOMO with the  $f_{LUMO-HOMO}$  being 0.4657 and  $C_{LUMO-HOMO}$  being 0.50516. The calculated results are verified by the experimental observation. From the experimental data, the main absorption bands of PYTPY in THF solution was captured at 327 nm and 277 nm as shown in Figure 3d. The optimal emission wavelength appeared at 383 nm as shown in Figure 3e. The experimental results fit well with that of the calculated data, which mean that our calculated method for predicting the electron transition performance in monomer state is reasonable.

The electron absorption property of PYTPY in dimer state is also calculated. The regulation of packing model with the lowest single point energy was selected from the results mentioned above. The calculated results is also listed in Table 3, which shows a main transition band centered at  $\lambda_{abs} = 367.37$  nm that is from HOMO-9 orbit to LUMO+1 orbit with the  $f_{(HOMO-9)-(LUMO+1)}$  being 0.0014 and  $C_{(HOMO-9)-(LUMO+1)}$  being 0.66732. Another transition band is calculated at  $\lambda_{abs} = 298.60$  nm with the  $f$  value being 0.0227, the major contributors of which are quite complicated that is listed in Table 3. The electron cloud distributions of the dimer at different energy level are listed in Figure S12. In the HOMO-9 orbit, the electron is mainly located at the terpyridine unit of the calculated fragment 1 as shown in Figure 2a, which is mainly located throughout the whole molecule of fragment 1 as for LUMO+1 orbit and partly located at the C=C double bond of fragment 2. The results also reveal the intramolecular transfer process when the aggregated dimer is excited. The experimental result (Figure 3d-e) obtained in THF-H<sub>2</sub>O mixed solution shows two main absorption bands centered at 368 nm and 296 nm, which are very close to that of 367.37 nm and 298.60 nm, respectively.

**Table 3** Some of calculated excitation energies (E), oscillator strengths (f), corresponding wavelengths ( $\lambda_{abs}$ ) and major contributors for molecular monomer and dimer based on bp86/cc-pvtz.

	E (eV)	$\lambda$ (nm)	f	composition (C)
absorption for monomer	3.8037*	325.96	0.2516	102(H <sub>1</sub> -6)→109(L <sub>1</sub> ) (0.56068)
	4.4336*	279.65	0.2020	98(H <sub>1</sub> -10)→109(L <sub>1</sub> ) (0.43994)
fluorescence for monomer	3.2604*	380.27	0.4657	109(L <sub>1</sub> )→108(H <sub>2</sub> ) (0.50516)
absorption for dimer	3.3749*	367.37	0.0014	207(H <sub>2</sub> -9)→218(L <sub>2</sub> +1) (0.66732)
	4.1522	298.60	0.0227	197(H <sub>2</sub> -19)→217(L <sub>2</sub> ) (0.13123)
				197(H <sub>2</sub> -19)→218(L <sub>2</sub> +1) (0.43135)
				198(H <sub>2</sub> -18)→218(L <sub>2</sub> +1) (0.15319)
				211(H <sub>2</sub> -5)→223(L <sub>2</sub> +6) (0.40032)

\* main transition

As discussed above, the experimental data for PYTPY in monomer and dimer states fit well with the calculated results, which also reveals that this simply calculation method to forecast the intramolecular charge transfer performance in dilute THF and/or

THF-H<sub>2</sub>O mixed solution is reasonable that can be used to study other organic materials in other solvents. DOI: 10.1039/C8CE01940A

### 3.3 The influence of acidity on the aggregation, morphology and electron transition

In 2018, Valverde et al. reported the self-assembly kinetics of  $\pi$ -conjugated amino acids at micro and/or nanoscale. They found that this type of molecule can self-assemble into long fibers upon protonation in an acidic environment, due to the protonation-induced nucleation by monomeric addition followed by subsequent stages of aggregation and elongation [31]. Here, we consider that PYTPY molecule possesses four pyridine rings that can interact with H<sup>+</sup>, which will then influence the intermolecular interactions and the related aggregation process. Thus, the influence of acidic environment on the self-aggregation style and the related aggregated morphology of PYTPY was studied.

#### 3.3.1 The effect of 1 and/or 3 equivalents of H<sup>+</sup> on the aggregation forces

Considering the reactive activity of different pyridine units and the spatial resistance effect, the selected molecular model for 1 positive charge was added at N atom of the pyridine unit (cycle ① in Scheme 1), which is shown in Figure 4a and optimized through b3lyp/6-31g level basis. The dimer's molecular models along different directions were also constructed from the CIF data (Figure 2) and was optimized through b3lyp/6-31g(d) method. The optimized model are showed in Figure 4b-d. The very first driving force in acid medium for self-aggregation is attributable to coulombic forces between positive charged pyridine group and the opposite charged ions. Exploiting these properties, the possibility to form aggregates of free positive charged PYTPY molecules has been demonstrated, which is responsive to pH variation or H<sup>+</sup> equivalent. Here, different H<sup>+</sup> equivalents (from 1 to 3 equiv.) are chosen to simplify calculation model and/or reduce calculation time.

The calculation results show that the single point energy of one positive charged PYTPY molecule is -1297.61779989 a.u. The energies of PYTPY dimer under 1 equiv. of H<sup>+</sup> existence along three different directions are -2595.44411806, -2595.40870835 and -2595.43649565 a.u., respectively. The relative binding energy is 1.00: 0.83: 0.96. That is to say, the assembling energies along different directions are similar to each other with the minimum difference being 4%. The results mean that PYTPY molecules have tendency to aggregate into three-dimensional structures in 1 equivalent of H<sup>+</sup>.

The effect of 2 equivalents H<sup>+</sup> on the PYTPY aggregation is shown in ESI. The selected molecular model for 2 positive charge was added at N atom of the pyridine unit ① and ④ according to spatial resistance effect as shown in Figure S15. In the following part, the effect of 3 equivalents H<sup>+</sup> will be discussed in detail.

Considering the spatial resistance effect and the repulsive interaction between charged molecules, the selected molecular model for 3 positive charge was added at N atom of the pyridine unit ①, ② and ③, which is shown in Figure 4e. The 3 positive charged dimer's models were optimized through b3lyp/6-31g(d) method. The optimized structures of the dimer are listed in Figure 4e-h. The detailed construction process of the models is as follows. The interaction between adjacent protonated tripyridine units is used to construct the first dimer's model as shown in Figure 4f. The interaction between the benzene unit and one of the pyridine unit of the protonated tripyridine unit (② or ③) is used to construct the second model as shown in Figure 4g. The interaction between

pyridine unit ④ and one of the pyridine unit of the protonated tripyridine unit (② or ③) is used to construct the third model (Figure 4h). These three types of dimer include the basic types of interaction between adjacent 3 positive charged acidified molecules. The single point energy of 3 positive charged molecule monomer and the dimers was also calculated through b3lyp/6-31g(d) method. The calculated single point energy of 3 positive charged molecular monomer is -1298.92678021 a.u., which is -2598.35840314, -2598.53703945 and -2598.04008762 a.u. for the dimers at three directions, respectively. The relative binding energy is calculated to be 2.71: 3.66: 1.00. The relative binding energy along the direction of Figure 4g is higher than that of the other two. The results mean that when 3 equivalents of  $H^+$  are added into PYTPY solution, the aggregated morphology may be one-dimensional structure, possibly grows according to the staking style as shown in Figure 4g. The results are reasonable that the exclusion effect between protonated pyridine units may decrease the interaction strength between adjacent protonated molecules, while the attraction effect between protonated pyridine unit and multi-electron conjugated benzene unit is the main character, which lead to higher interaction force of model Figure 4g than that of 4f. Furthermore, the molecules in model 4h exhibits a twisted interaction structure that will decrease the interaction strength. That is to say, the interactions between adjacent molecules in model 4g show the strongest strength.

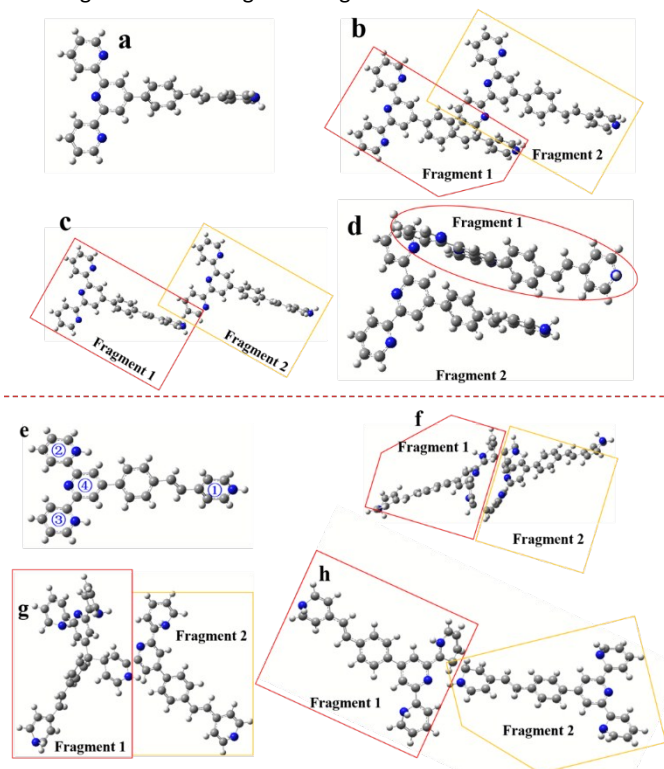


**Figure 4** (a-d) Fragments selected from simulated structure after acidification by 1 equivalent of  $H^+$  ion for calculation of (a) single molecule and weak interactions along different directions. (e-h) Fragments selected from simulated structure after acidification by 3 equivalents of  $H^+$  ion for calculation of (e) simulated single molecule and weak interactions.

Form the discussions mentioned before, different equivalents of  $H^+$  may bring about different aggregation forces. When 1 equivalents of  $H^+$  is added, the forces along different directions may

similar to each other. When more dosage of  $H^+$  is added, the force along one direction will increase, which will be beneficial for 1-D aggregation. To make sure the reasonableness of such predictions, the aggregated morphology was checked from scanning electron microscope (SEM) images.

### 3.3.2 The morphology under different equivalents of $H^+$

Indeed, the theoretical calculation results are well validated by experiments. When PYTPY-THF solution was added with different equivalents of hydrochloric acid, the morphology of PYTPY assembly changed violently as shown in Figure 5. The equivalents of hydrochloric acid was changed from 1 to 4.

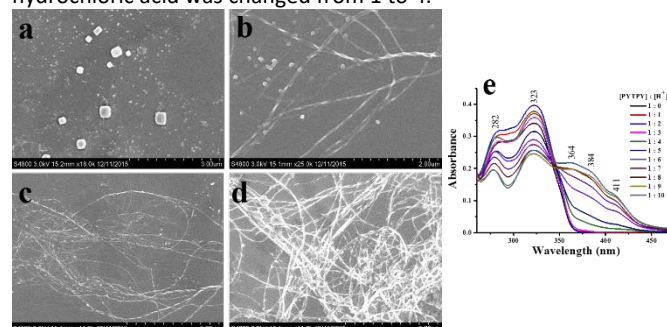


**Figure 5** SEM images of PYTPY aggregates formed under different equivalent of  $H^+$ . (a): 1, (b): 2, (c): 3 and (d): 4 equivalents. (e) UV-vis spectra of PYTPY in THF solution when different equivalents of  $H^+$  were added

When 1 equivalent of  $H^+$  is added, PYTPY molecules tend to aggregate into blocky structure (Figure 5a), the size of which ranges from 200 nm to 300 nm. Compared to the results got from THF- $H_2O$  solution (Figure 3), the blocky structure in this condition clearly indicates the strong influence of additional  $H^+$  ion on the self-assembly process of PYTPY. As free PYTPY molecules tend to form 1-D structure (as discussed in Part 3.2), when  $H^+$  is added, the pyridine ring near the C=C double bond will be acidulated firstly, and increases the electron acceptor strength of pyridine unit ① and decrease the intramolecular charge transfer strength of the whole PYTPY molecule, which then decrease the dipole-dipole interactions between adjacent acidulated PYTPY molecules. Thus, the 1-D growth dynamic decrease and the as-observed rod-like structure (Figure 3) disappears. The relative enhanced interactions along the other two dimensions make acidulated PYTPY molecules self-assembly into 3-D blocky structure in assistance of 1 equivalents of  $H^+$ . Further, when the equivalent of  $H^+$  is increased, the 3-D blocky structures are connected together to form 1-D wires. Because the reactivity of N atom at cycle ① with  $H^+$  is higher than that at cycle ② and/or ③, blocky structures may always appear when more equivalent of  $H^+$  is added. Indeed, some blocks appear on the nodes of the wire as shown in Figure 5b-d. Thus, it can be concluded that the formation mechanism of 1-D wires observed in acid solution was different from the 1-D rods obtained in neutral water medium. Combined with theoretical calculations, it is thought that 1-D wires in acid solution is constructed due to homologous  $\pi$ - $\pi$  interactions as shown in Figure 4g and 2d, and that C2-H2...N4 intermolecular hydrogen bond can lead molecules grow along  $a$  axis to form 1-D rods in pure water.

### 3.3.3 The calculated and experimental UV-vis absorption under different equivalents of $H^+$

The electronic structure and transition performance of PYTPY under 1 or 3 equivalents of  $H^+$  was investigated at the b3lyp/cc-pvtz level basis set, both for acidified monomer and dimer. The molecular geometry used for the acidified dimer was the same as

that used for the lowest single point energy calculation (Figure 4b and 4g). As for PYTPY-1H<sup>+</sup> monomer, the theoretical result shows two main transitions as  $\lambda_{\text{abs}} = 367.71$  nm and 277.55 nm, respectively. As for the PYTPY-1H<sup>+</sup> dimer, there exists an absorption band at 368.14 nm from HOMO-2 orbit to LUMO+3 orbit with  $f$  value being 0.1571. At the same time, the  $f$  value at 324.55 nm is calculated as 0.0008, which means that the absorption band at this energy gap is very weak. Moreover, a new absorption band centered at 403.20 nm appears which is transitioned from the HOMO-2 orbit to the LUMO+1 with  $C_{(\text{HOMO-2})-(\text{LUMO+1})}$  being 0.69974. The new band is considered as coming from the increased electron accepting strength of the protonated pyridine unit and the corresponding enlarged  $\pi$ -conjugated structure, which may also appear when the equivalents of H<sup>+</sup> is increased. Further, as the protonated saturation of pyridine unit is one, this absorption wavelength will be kept at around 410 nm when the equivalents of H<sup>+</sup> is more than one. Indeed, when we simulated the equivalents of H<sup>+</sup> as three, the transition at  $\lambda_{\text{abs}} = 411.22$  nm exists for the aggregated dimer.

The calculated results are verified by the experimental measurements to check the feasibility of the calculation method and the accuracy of the modelling structures for the protonated PYTPY. In THF solution, when different equivalents of hydrochloric acid are added, the absorption bands at 323 nm and 282 nm shows an increase trend firstly and then a decrease trend (Figure 5e). Meanwhile three new bands centred at 364 nm, 384 nm and 411 nm appear (Figure 5e), which gradually increase and exhibit slightly change only after the equivalent is larger than 7.0. The experimental conclusions are consistent with the predicted results, which are reasonable that when hydrochloric acid is added into the THF solution of PYTPY, the pyridine unit of cycle ① is protonated firstly and changed the  $\pi$ -conjugated molecule. At the same time, the terpyridine group at the other end of the structure will be protonated after 1.0 equivalent, which may cause a stronger electron acceptor strength. The result is the appearance of absorption bands at longer wavelength (from 360 nm to 410 nm). When the equivalent is larger than 2.0, the repulsive force between adjacent protonated-PYTPY molecules will be strong and prevent further protonation of the molecule, which may lead the subtle changes of absorption band and/or absorbance value at around 360-410 nm. Also, we must realize that when the first drop of hydrochloric acid is added into the studied system, the protonation process of both terpyridine and pyridine units will occur at the same time. So the decrease of absorbance at 323/282 nm and the increase at 360-410 nm exhibit gradual change.

The results examined and discussed in acid media give us confidence to study the aggregation style and the related optical performance in coordination environment when metal ions are added into the system.

### 3.4 The influence of silver ion on the self-aggregation

Pyridine derivatives are reliable candidates to employ molecular building blocks with self-assembly structures due to supramolecular scaffolds through either non-covalently or covalently interactions [32]. As there exists terpyridine group with strong coordination ability, PYTPY will be coordinated with metal ions, which will bring about violent changeable morphology, the related optical

properties such as UV-vis absorption will be tuned along with the changeable morphology. In the past decade, terpyridine derivatives have generated a wide-range of supramolecular architectures through coordinating effect with some types of metal ions, such as Zn<sup>2+</sup>, Cd<sup>2+</sup>, or Ru<sup>2+</sup> [33-34]. In this part, silver ion was chosen through the hard-soft-acid-base theory, as its common coordination number is four which make silver ion simply link two PYTPY molecules in one complex cell [35]. THF-H<sub>2</sub>O was chosen as the mixed solvent because silver ion cannot be reduced by THF.

The optimized dimer under Ag<sup>+</sup> ion existence was shown in Figure 6, which was optimized through b3lyp/6-31g\* method. The detailed modelling was described in the labelling of Figure 6. Ag<sup>+</sup> ion was located at the position to link two pyridine groups from adjacent molecules as Figure 6a, link pyridine group of one molecule and terpyridine group of adjacent molecule as Figure 6b, link terpyridine group of one molecule and  $\pi$ -conjugated electrons of styrene unit at adjacent molecule as Figure 6c. Similar to the construction of 3 positive charged dimers, the location of Ag<sup>+</sup> ion covered all of the possible ways of weak interaction. The related interaction energies were calculated through b3lyp/6-31g\* method. The single point energies of the dimers shown in Figure 6a-c was -2595.93115778, -2595.95707570 and -2595.72817679 a.u., respectively. The relative binding energy along different directions were calculated as 0.98: 1.00: 0.84. The results were reasonable that the four coordination number of Ag<sup>+</sup> ion can make it link the three N atoms of terpyridine unit and one N atom of pyridine unit. Also, there existed coordination effect between Ag<sup>+</sup> ion and conjugate electrons with moderate strength. The results also meant that the aggregated PYTPY molecules under Ag<sup>+</sup> existence may construct three dimensional structure at macro scale. Considering the related larger volume of Ag<sup>+</sup> ion than that of H<sup>+</sup> ion, the aggregated structure may also exist as zero-dimensional structure at nanoscale, as spatial steric hindrance effect of Ag<sup>+</sup> ion can obstruct the effective aggregation of PYTPY molecules. As shown in Figure 7a, when 1 equivalent of Ag<sup>+</sup> ion was added, the morphology of PYTPY under Ag<sup>+</sup> circumstance showed curly nanowires with length of about dozens of micrometers and width of about dozens of nanometers, which did not match with the calculated results. So we check the morphology through TEM image as shown in Figure 7b. It can be observed that the curly nanowires were composed of some tiny nanoparticles with the size of about 3-5 nm, that is to say PYTPY molecules tended to form zero-dimensional structure. To preclude the possible existence of Ag nanoparticles, XRD pattern was examined which did not support existence of Ag(0). So the observed morphology of PYTPY in Ag<sup>+</sup> addition confirmed the calculation results. Maybe, the existence of Ag<sup>+</sup> ions at the side of PYTPY molecule obstructed aggregation of PYTPY, but can link the zero-dimensional PYTPY aggregation particles together, then form prolonged structure. This speculation was reasonable that Ag<sup>+</sup> ions existed all around the studied system and the nanowires appeared all around the field of vision.

The possible aggregated style of PYTPY under Ag<sup>+</sup> existence was used to calculate the absorbing performance through bp86/6-311g\* method, the results are listed in Table 4. The main transition of PYTPY dimer under Ag<sup>+</sup> ion existence appears at 3.6688 eV, corresponding to 337.94 nm, which come from the electron transition between HOMO-8 orbit and LUMO+3 orbit. At HOMO-8

orbit of PYTPY dimer under  $\text{Ag}^+$  ion existence, the electron cloud density is mainly concentrated at the terpyridine unit at one

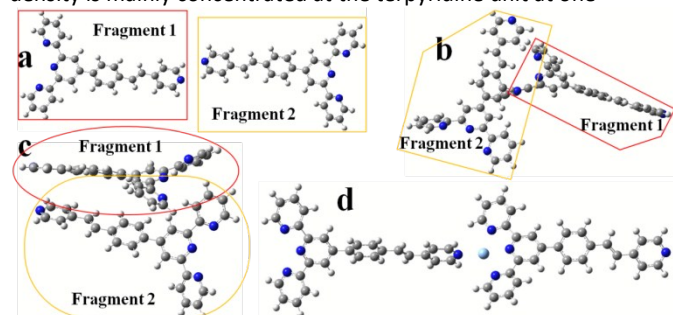


**Figure 6** Fragments selected from simulated structure at existence of 1 equivalent  $\text{Ag}^+$  ion for calculation weak interactions when  $\text{Ag}^+$  linked (a) two pyridine groups from adjacent molecules, (b) pyridine group of one molecule and terpyridine group of adjacent molecule, (c) terpyridine group of one molecule and  $\pi$ -conjugated electrons of styrene unit at adjacent molecule, (d) simulated structure of PYTPY-Ag complex upon calculation results

molecule and the pyridine unit at adjacent molecule. While for LUMO+3 orbit, the electron cloud is dispersed at the whole conjugated structure of one PYTPY molecule. The experimental data shows a main UV-vis absorption band at 335 nm (Figure 7e), matches well with the calculated result.

In the experiment, we noticed that the redox properties of the solvent influences the morphology. For example, when DMF with reducing performance was used as the solvent,  $\text{Ag}^+$  ions can be reduced to  $\text{Ag}^0$  and form Ag nanoparticles. The phenomenon also reveals the effect of  $\text{Ag}^+$  ion on the morphology of PYTPY. When  $\text{Ag}^+$  ion is existed in the system, the morphology of PYTPY changes violently from nanorod to nanowire composed of zero-dimensional tiny particles. When  $\text{Ag}^+$  ion is reduced to  $\text{Ag}^0$  by DMF, the morphology of PYTPY still showed rod-like morphology with only slight change on the size. Moreover, it can be observed that some Ag particles appears at the surface of PYTPY nanorods as shown in Figure 7c. Furthermore, when temperature is increased to boiling point of DMF ( $\sim 153^\circ\text{C}$ ), and the mixed solution is refluxed overnight, the PYTPY-Ag complex may formed. The related morphology of PYTPY-Ag complex is shown in Figure 7d, some thin spindle structure is observed, with the length of  $\sim 2\ \mu\text{m}$ , the width of hundreds of nanometers and the thickness being dozens of nanometers. Also, there do not exist any tiny Ag nanoparticles that are stuck at the surface of the thin spindles. The XRD pattern do not show the existence of  $\text{Ag}^0$  for this sample (Figure S23). The results also reveal the different reaction speed and reaction mechanism. When the temperature was low ( $80^\circ\text{C}$  e.g.) and the reaction time was short (30 min), DMF reduced  $\text{Ag}^+$  to  $\text{Ag}^0$  [36]. While at higher temperature (boiling point), the reaction speed of PYTPY with  $\text{Ag}^+$  to construct PYTPY-Ag complex was faster than that of reducing reaction to  $\text{Ag}^0$ , so PYTPY-Ag complex was formed at higher temperature [37]. However, this reaction need longer time, so  $>12$  hours was taken.

In the following part, the model of PYTPY-Ag complex was used for controlled calculation. The experimental and calculated results for  $\text{Ag}^+$  induced PYTPY molecules' aggregation reveal the possible coordination style of PYTPY-Ag complex. The main possible coordination mode may exist at pyridine group and terpyridine group. Thus, the structure of PYTPY-Ag complex is simulated upon

calculation results as shown in Figure 6d, in which  $\text{Ag}^+$  ion is attached to terpyridine unit of one PYTPY molecule and pyridine unit of another molecule through coordination bond to construct PYTPY-Ag crystal cell. The UV-vis absorption band and the related electron cloud density distribution of PYTPY-Ag complex for controlled analysis are analyzed through b3lyp method. The metal center  $\text{Ag}(\text{I})$  has been described by the lan12dz effective core potential (ECP) basis set while non-metal atoms by the cc-pvtz basis set.

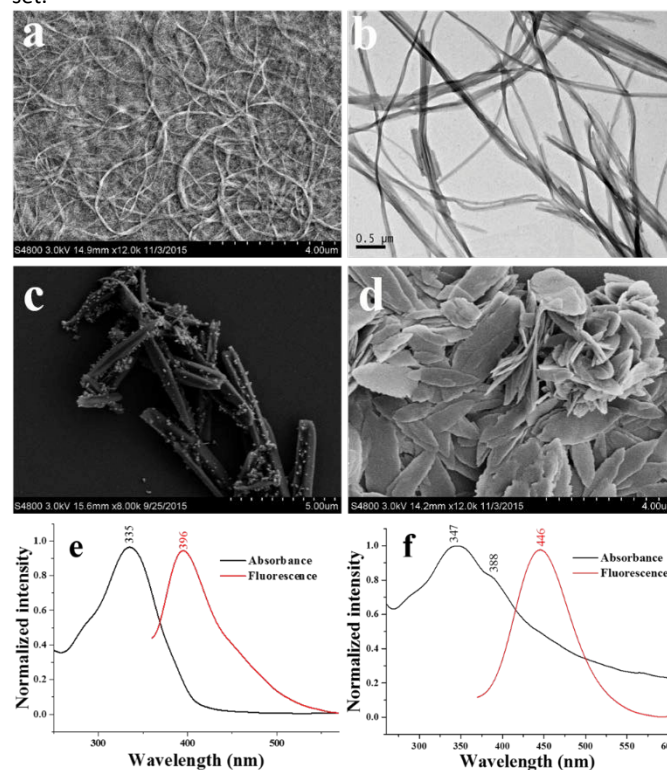


**Figure 7** (a-d) Morphology of samples prepared under different conditions when  $\text{AgNO}_3$  was added into the studied system. (a) SEM image of PYTPY samples when 1 equivalent of  $\text{AgNO}_3$  was added into PYTPY-THF solution, (b) TEM image of PYTPY samples when 2 equivalents of  $\text{AgNO}_3$  were added into PYTPY-THF solution, (c-d) SEM image of PYTPY samples when 3 equivalents of  $\text{AgNO}_3$  were added into PYTPY-DMF solution (c) under violently stirring at  $80^\circ\text{C}$  for 30 min, (d) refluxed overnight. (e-f) Normalized UV-vis absorption and fluorescence spectra of: (e) PYTPY aggregates when 1 equivalent of  $\text{Ag}^+$  ion was added, (f) PYTPY-Ag complex obtained from refluxed DMF solution.

For the simulated PYTPY-Ag complex, the main transition appears at 3.2207 eV, corresponding to 384.96 nm, which come from the electron transition between HOMO-4 orbit and LUMO+1 orbit. At HOMO-4 orbit (Figure S20), the electron cloud is mainly concentrated at the whole conjugated structure of one PYTPY molecule and partly located at the  $\text{Ag}^+$  ion. For the LUMO+1 orbit, the electron cloud is mainly concentrated at pyridine unit of the same PYTPY molecule at HOMO-4 orbit, the C=C double bond and connected benzene unit. There also exists some electron cloud distribution at the  $\text{Ag}^+$  ion. The results mean that the electron excited process of PYTPY-Ag complex is also accompanied by the electron cloud re-distribution, which can adjust intramolecular charge transfer here. The experimental UV-vis absorption data of PYTPY-Ag complex exhibits a wide band from 300 nm to 550 nm, the main absorption band centers at 347 nm and a shoulder band appears at 388 nm band (Figure 7f). The 347 nm absorption band may come from the characteristic absorption of PYTPY, which

shows an obviously red-shift by 20 nm from 327 nm of free PYTPY molecule (Figure3d), and 12 nm red-shift from 335 nm of PYTPY under Ag<sup>+</sup> ion existence (Figure7e). The coordination effect between Ag<sup>+</sup> ion and PYTPY may enlarge the  $\pi$ -conjugated degree and results in the red-shifted absorption. Furthermore, the 388 nm band is considered as coming from the intrinsic absorption of the complex, which is consistent with theoretical calculations.

**Table 4** Some of calculated excitation energies (E), oscillator strengths (f), corresponding wavelengths ( $\lambda_{\text{abs}}$ ) and major contributors for PYTPY in dilute THF solution when 1 equivalent Ag<sup>+</sup> ion was added

	E (eV)	$\lambda$ (nm)	f	composition (C)
absorbance for PYTPY when Ag <sup>+</sup> existed	3.6688*	337.94	0.0454	208(H <sub>7</sub> -8) → 220(L <sub>7</sub> +3) (0.582221)
absorbance for PYTPY-Ag complex	3.5801	346.31	0.0009	220(H <sub>8</sub> -5) → 228(L <sub>8</sub> +2) (0.69082)
	3.2207*	384.96	0.6292	221(H <sub>8</sub> -4) → 227(L <sub>8</sub> +1) (0.61042)

\* main transition

## 4 Conclusion

In summary, this study used the computational calculation method to understand the influence of external conditions on the intermolecular interaction between adjacent molecules of the target terpyridyl derivative PYTPY. The simulated structure of PYTPY under the existence of water, Ag<sup>+</sup> ion and different equi. of H<sup>+</sup> ion brought about different types of intermolecular interactions that resulted in changeable morphology and tunable absorption band. The calculated aggregation state and absorbing performance fit well with that captured at experimental results. This simply calculation method can give us an opportunity to understand the weak intermolecular interactions, the possible aggregate style and morphology, which affords insight into tailoring the self-assemble process, and can also study the main transitions between the ground states and the excited states of an organic compound under different external conditions. Based on such results, the possible optical performance of an organic compound can be premastered to guide the design, preparation, experiments and applications.

## Acknowledgements

The authors thank Dr. Hui Wang at Wannan Medical College, Dr. Kun Wang and Dr. Hai-Zhu Yu at AnHui University for helpful suggestions and discussions. This work was supported by the Natural Science Foundation of Anhui Province of China (1508085SMB208), the Educational Commission of Anhui Province of China (KJ2016A788) and the NSFC (No. 51673001, 51472002).

## Notes and references

- ‡ The crystallographic data of PYTPY: CCDC 1870772.
- R. Zou, J. Zhang, S. Z. Hu, F. Hu, H. Y. Zhang, Z. Y. Fu, *CrystEngComm*, **2017**, *19*, 6259; DOI: 10.1039/C6CE01940A
  - Q. Zhang, J. Su, D. Feng, Z. Wei, X. Zou and H. C. Zhou, *J. Am. Chem. Soc.*, **2015**, *137*, 10064;
  - Q. Benito, I. Maurin, M. Poggi, C. Martineau-Corcos, T. Gacoin, J. P. Boilot, S. Perruchas, *J. Mater. Chem. C*, **2016**, *4*, 11231
  - M. R. Elmersy, R. Su, A. A. Fadda, H. A. Etman, E. H. Tawfik, A. El-Shafei, *Dye Pigm.*, **2018**, *158*, 121;
  - X. J. Zhang, X. H. Zhang, K. Zou, C. S. Lee and S. T. Lee, *J. Am. Chem. Soc.*, **2007**, *129*, 3527
  - J. C Bolinger, M. C. Traub, J. Brazard, T. Adachi, P. F. Barbara, D. A. Vanden Bout, *Acc. Chem. Res.*, **2012**, *45*, 1992
  - L. R. Valverde, B. A. Thurston, A. L. Ferguson, W. L. Wilson, *Langmuir*, **2018**, *34*, 7346
  - M. R. Molla, M. A. Rub, A. Ahmed, M. A. Hoque, *J. Mole. Liq.*, **2017**, *238*, 62
  - S. Singh, A. Bhadoria, K. Parikh, S. K. Yadav, S. Kumar, V. K. Aswal, S. Kumar, *J. Phys. Chem. B*, **2017**, *121*, 8756
  - Y. Sagara, T. Kato, *Nat. Chem.*, **2009**, *1*, 605
  - H. X. Liu, J. Lu, T. Zheng, D. M. Liu, F. Y. Cui, *Environ. Eng. Sci.*, **2018**, *35*, 846
  - M. Humbert-Droz, C. Piguat, T. A. Wesolowski, *Phys. Chem. Chem. Phys.*, **2016**, *18*, 29387;
  - T. W. Bell, P. J. Cragg, A. Firestone, A. D. I. Kwok, J. Liu, R. Ludwig, A. Sodoma, *J. Org. Chem.*, **1998**, *63*, 2232;
  - A. Wild, A. Winter, F. Schlütter, U. S. Schubert, *Chem. Soc. Rev.*, **2011**, *40*, 1459
  - H. J. Bolink, L. Capelli, E. Coronado and P. Gavina, *Inorg. Chem.*, **2005**, *44*, 5966
  - F. Ibersiene, C. Latouche, C. Katan, A. Boucekkine, *Phys. Chem. Chem. Phys.*, **2018**, *20*, 7401
  - A. O. Adeloye, P. A. Ajibade, *Sci. World J.*, **2014**, 570864
  - Y. Z. Zhang, H. W. Yang, S. Guan, Z. H. Liu, L. Y. Guo, J. W. Xie, J. B. Zhang, N. N. Zhang, J. Song, B. Zhang, Y. Q. Feng, *Dyes Pigm.*, **2018**, *157*, 6
  - T. T. Wang, J. L. Zhang, H. M. Hu, Y. Cheng, L. L. Xue, X. F. Wang, B. Z. Wang, *Polyhedron*, **2018**, *151*, 43
  - A. Maroń, K. Czerwińska, B. Machura, L. Raposo, C. Roma-Rodrigues, A. R. Fernandes, J. G. Mafecki, A. Szlapa-Kula, S. Kula, S. Krompiec, *Dalton Trans.*, **2018**, *47*, 6444
  - F. Ishiwari, Y. Shoji, T. Fukushima, *Chem. Sci.*, **2018**, *9*, 2028
  - M. R. Elmersy, R. Su, A. A. Fadda, H. A. Etman, E. H. Tawfik, A. El-Shafei, *Dyes Pigments*, **2018**, *158*, 121
  - D. Spitzer, V. Marichez, G. J. M. Formon, P. Besenius, T. M. Hermans, *Angew. Chem.*, **2018**, *130*, 11519
  - R. M. Richard, B. W. Bakr, C. D. Sherrill, *J. Chem. Theory Comput.*, **2018**, *14*, 2386
  - S. S. Yu, Y. T. Yang, T. Chen, J. Z. Xu, L. Y. Jin, *Nanoscale*, **2017**, *9*, 17975
  - L. Kong, J. X. Yang, L. J. Cheng, P. Wang, H. P. Zhou, J. Y. Wu, Y. P. Tian, B. K. Jin, X. T. Tao, *J. Mole. Struct.*, **2014**, *1059*, 144
  - S. Singh, A. Bhadoria, K. Parikh, S. K. Yadav, S. Kumar, V. K. Aswal, S. Kumar, *J. Phys. Chem. B*, **2017**, *121*, 8756
  - L. Kong, J. X. Yang, Z. M. Xue, H. P. Zhou, L. J. Cheng, Q. Zhang, J. Y. Wu, B. K. Jin, S. Y. Zhang, Y. P. Tian, *J. Mater. Chem. C*, **2013**, *1*, 5047
  - M. Humbert-Droz, C. Piguat, T. A. Wesolowski, *Phys. Chem. Chem. Phys.*, **2016**, *18*, 29387
  - A. Wild, A. Winter, F. Schlütter, U. S. Schubert, *Chem. Soc. Rev.*, **2011**, *40*, 1459
  - L. R. Valverde, B. A. Thurston, A. L. Ferguson, W. L. Wilson, *Langmuir*, **2018**, *34*, 7346
  - F. Ishiwari, Y. Shoji, T. Fukushima, *Chem. Sci.*, **2018**, *9*, 2028
  - T. Z. Xie, Y. C. Yao, X. Y. Sun, K. J. Endres, S. Y. Zhu, X. L. Wu, H. Li, J. M. Ludlow III, T. B. Liu, M. Gao, C. N. Moorefield, M.

## ARTICLE

## Journal Name

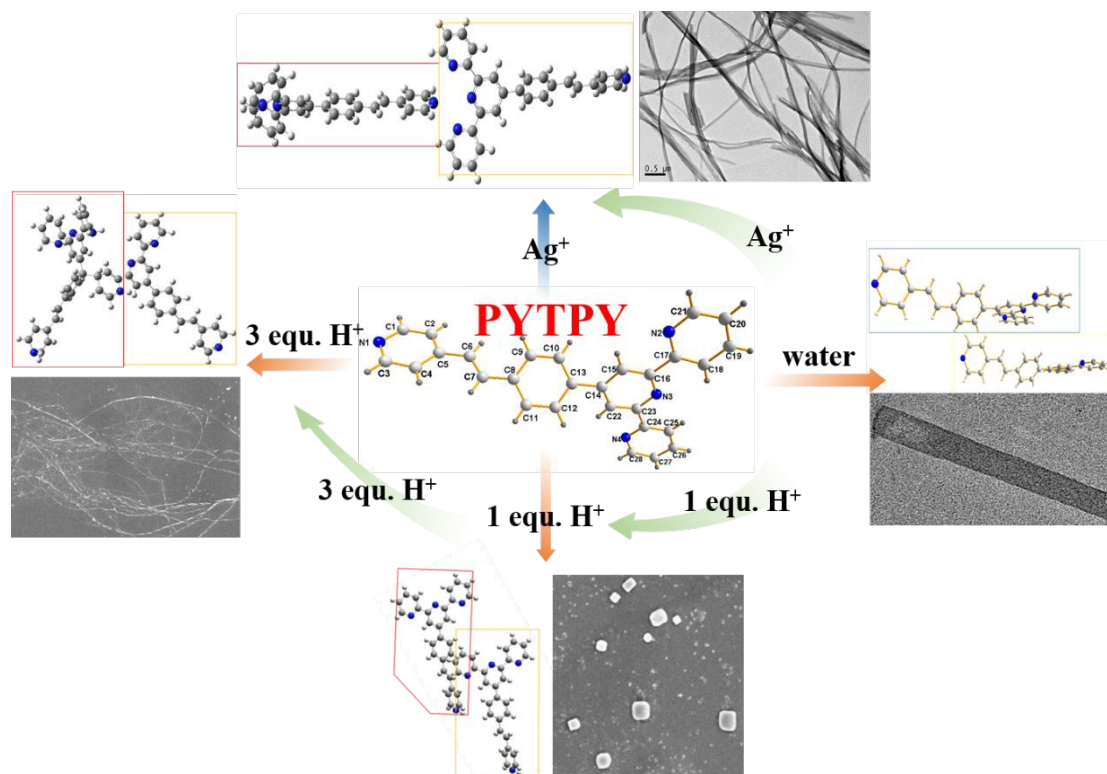
- J. Saunders, C. Wesdemiotis, G. R. Newkome, *Dalton Trans.*, **2018**, 47, 7528
- 34 L. Wang, Z. Zhang, X. Jiang, J. A. Irvin, C. L. Liu, M. Wang, X. P. Li, *Inorg. Chem.*, **2018**, 57, 3548
- 35 S. Del Piero, R. Fedele, A. Melchior, R. Portanova, M. Tolazzi, E. Zangrando, *Inorg. Chem.*, **2007**, 46, 4683
- 36 J. G. Piao, F. Gao, Y. Li, L. Yu, D. Liu, Z. B. Tan, Y. J. Xiong, L. H. Yang, Y. Z. You, *Nano Research*, **2018**, 11, 3193
- 37 T. Lu, C. F. Yang, C. A. Steren, F. Fei, X. T. Chen, Z. L. Xue, *New J. Chem.*, **2018**, 42, 4700

View Article Online  
DOI: 10.1039/C8CE01940A

Graphical abstract for:

**Understanding the molecular orientation growth at nanometer scale and adjustable electron transition performance of a terpyridyl derivative under different external environments**

Hai-Yan Wang, Lin Kong, Shu-Juan Zhu, Hong-Ping Zhou, Jia-Xiang Yang



TD-DFT calculation is used to forecast the aggregation style of TPYPY under different external additions, predict the related morphology and electron transition performance.